Renewable and Sustainable Energy Reviews 32 (2014) 983–993

Contents lists available at ScienceDirect

Renewable and Sustainable Energy Reviews

journal homepage: www.elsevier.com/locate/rser

Solar electricity generation across large geographic areas, Part II: A Pan-American energy system based on solar

Wolf D. Grossmann [a,b], Iris Grossmann [c,*], Karl W. Steininger [a,d]

[a] Wegener Center for Climate and Global Change, University of Graz, Leechgasse 25, A-8010 Graz, Austria
[b] International Center for Climate and Society, University of Hawaii at Manoa, 1680 East–West Road, Honolulu, HI 96822, USA
[c] Center for Climate and Energy Decision Making, Carnegie Mellon University, 5000 Forbes Ave, Pittsburgh, PA 15213, USA
[d] Department of Economics, University of Graz, Universitaetsstrasse 15, A-8010 Graz, Austria

ARTICLE INFO

Article history:
Received 14 December 2011
Received in revised form
25 November 2013
Accepted 4 January 2014
Available online 4 February 2014

Keywords:
Review of large-scale solar energy network
Renewable energy
US super grid
Solar intermittency
Hourly insolation data
Pan-American grid
Substitution between generation capacity and storage

ABSTRACT

Due to the rapid decrease of the costs of photovoltaics, large schemes for solar electricity generation have recently been suggested. The new method of isolines or contour lines between generation capacity and storage for a specific load allows a thorough review of these schemes. Such a review is necessary given that the costs of photovoltaics have been and are decreasing much more rapidly than the costs of storage. We apply this method to the "Solar Grand Plan" proposed by Zweibel, Fthenakis and Mason. The Grand Plan connects only a small number of time zones and is restricted to the northern hemisphere. Schemes recently suggested, e.g., for the Asian–Australian region would connect both hemispheres. In such spatially extended schemes the substitutability between generation capacity and storage can be extended to also include transmission lines. We review the Grand Plan against the background of several spatially extended Pan-American schemes and show how major drawbacks of the Grand Plan with respect to overcapacity can be overcome based on hourly scaling of NASA Solar Sizer insolation data and optimization of the required generation capacity and storage. We then outline transmission lines for Pan-American networks, transmission costs, projected solar electricity costs, and line utilization rates. In addition to enabling significant cost savings through reduced overcapacity, Pan-American schemes enable revenue flows and improved availability of electricity that are favorable for economic development.

Contents

* Corresponding author. Tel.: +1 412 268 5489; fax: +1 412 268 3757.
E-mail address: irisg@andrew.cmu.edu (I. Grossmann).

1364-0321/$ - see front matter
http://dx.doi.org/10.1016/j.rser.2014.01.003

1. Introduction

Distributed solar electricity generation across large geographic areas [1–10] can significantly reduce the intermittency of solar energy [2,6,10–14]. In ever more regions such schemes become competitive due to rapidly decreasing costs of photovoltaics (PV). Research groups and large industrial consortia have suggested schemes such as Desertec EUMENA (connecting Europe, North Africa, and the Middle East) [3–5,7] and schemes that comprise Asia and Australia [6]. Most elaborated is the "Solar Grand Plan" [1,15] a predominantly renewable energy supply system using high insolation areas in the US Southwest. Due to low insolation in winter, the Grand Plan needs expensive overcapacity, long-term storage, and fossil-fuel based generation capacity during periods of low insolation. As a consequence, solar electricity is too expensive. We review the Grand Plan and discuss the reasons for these shortcomings.

Using the method of isolines between generation capacity (G) and storage (S) we show that at present costs of generation capacity and storage, the ratio of G to S should be increased to decrease overall costs. G–S-Isolines (or: contour lines between G and S) depict the curves along which a given load profile is met as a function of G and S [10]. They are the lower boundary of the feasible area of G and S that allows meeting a given load and hence provide an easy method to determine the minimal cost combination of G and S.

We next apply the method of G–S-Isolines to an extension of the Solar Grand Plan into a Pan-American scheme. This extension can operate with much lower overcapacity. The inclusion of sites on both hemispheres compensates for low insolation during winter on each hemisphere and allows a marked decrease of overcapacity compared to the Solar Grand Plan. Costs become competitive through an optimal selection of sites across North and South America. The optimization for effectively addressing intermittency needs hourly solar insolation values [11] for the American continent. Hourly values allow calculating the combined solar irradiation of multiple sites given their respective time zones, which then permits optimizing site selection as well as optimizing the required amounts of G and S. Hourly data are available only for North America and only for the relatively short time-span from 1991 to 2010 [16]. Using a recently developed method presented in the companion paper [10], daily NASA Solar Sizer insolation data [17] are converted to hourly resolution.

Section 2 briefly reviews the recent development in solar energy. Data and methods are discussed in Section 3. Section 4 reviews the Solar Grand Plan and implications for electricity prices. In Section 5, the Grand Plan is reviewed against Pan-American extensions. Several Pan-American configurations are discussed to illustrate the relative advantages of different types of sites, including high-latitude, subtropical desert, and tropical sites. To assess cost savings, three components of Pan-American concepts are discussed: (1) demand projections, (2) possible transmission lines and their current and possible future transmission costs, and (3) projected solar electricity costs. In Section 6 the results are presented, followed by a discussion in Section 7. We find that linking North and South American electricity generation and demand allows eliminating fossil fuels, which are used in the Solar Grand Plan, and drastically decreasing expensive long-term storage. Good availability of energy in its most valuable form, electricity, and resulting revenue flows could enhance economic development, in particular in remote areas in South America. The same method could be applied for reviewing and optimizing the Desertec EUMENA network [3,5,7] or the Asian–Australian schemes.

2. Background: Recent development of solar electricity

PV is the fastest growing electricity technology. Globally between 1976 and 2012, installed PV has grown by a factor of two every two years; the R^2 of this growth rate estimate is 0.94 [18]. With each doubling of installed capacity the cost of PV has decreased by 20% [18–20]. As a consequence the 2010s are predicted to be characterized by ongoing grid-parity events for 75–90% of the total global electricity market [19,21]. The cost of concentrating solar power (CSP) electricity is also decreasing, although much slower, so that its use in a large-scale plan for the US must be reassessed. Construction of large-scale solar installations has begun worldwide [22–26]. In 2013, three contracts for PV plants in Spain with 350 MW, 400 MW and 500 MW show this breakthrough in competitiveness [27]. For example, the 400 MW installation will cost \$571 m. With the annual insolation of Extremadura/Spain of 1730 kW h/m^2, this gives levelized costs of electricity (LCOE) from this plant of 8 ¢/kW h without subsidies (based on [28]). With the higher annual insolation of 2200 kW h/m^2 in the Sahara or the Mojave Desert, this installation would give electricity at 6.3 ¢/kW h which is, in 2014, almost the electricity costs of 6 ¢/kW h projected by Zweibel et al. [1] for 2020. Electricity costs of this installation in the Atacama Desert (Chile) with an annual insolation of ~2500 kW h/m^2 would be even lower at 5.5 ¢/kW h.

The rapid development of PV offers new options in dealing with pressing problems in the energy sector [1,2,22,23]. The Desertec Foundation plans to supply 80% of the electricity for 30 European countries from renewable energy by 2050, generated in Europe, the Middle East and North Africa [3–5,7]. Projected LCOE from CSP are €0.05 plus transmission costs of €0.015 in 2020, and of €0.04, plus €0.01, in 2050 [28]. The US Grand Plan would supply 69% of the US electricity needs and 35% of the total US energy needs (including transportation) from solar by 2050.

Our review uses G–S-Isolines to show that both the Desertec network and the US Solar Grand Plan require large amounts of over-capacity and storage. Other studies either also report very high over-capacity [29], or they do not explicitly resolve intermittency from variability and the diurnal cycle [9], or they do not aim to meet the entire load from renewables [11]. A recent study designed to meet 1/5 of the US electricity demand from solar and wind proposes over-capacity at up to three times the load [29]. Cost minimization requires minimizing the combination of G and S. This is possible through optimized site selection. Connecting time zones decreases the effects of day and night; connecting both hemispheres allows compensating for low insolation during winter on each hemisphere [10]. As both the Grand Plan and the Desertec EUMENA plan rely on few adjacent time zones, they need oversupply, storage and non-renewable electricity in winter to address day to day intermittency, low insolation in winter and worst-case conditions. The Grand Plan assumes fuel combustion on the order of 11.7% of the total energy consumed and storage of at least 258 TW h (compared to 6.7 terawatt (TW) of generation capacity).

3. Data and methods

20 years of daily NASA Solar Sizer insolation data for $1^\circ \times 1^\circ$ boxes on a horizontal surface [17] over the 20 years of 1986–2005 are used. These data are part of the NASA Surface meteorology and Solar Energy (SSE) Release 6.0, which were obtained from the NASA Science Mission Directorate's satellite and re-analysis research programs [30]. The surface solar insolation is inferred from satellite observations with the modified method of Pinker and Laszlo [31] using a radiative transfer model along with water vapor column amounts from the GEOS-4 product and ozone column amounts from satellite measurements. Satellite radiances are converted into broadband shortwave top of the atmosphere (TOA) albedos using angular distribution models from the Earth Radiation Budget Experiment [32]. The radiative transfer model is used to find the absolute value of the surface albedo which

produces a TOA upward flux that matches the TOA flux from the conversion of the clear-sky composite radiance. The years 1986–2005 represent a wide range of weather conditions including the major volcanic eruption of Mt. Pinatubo in 1991, which decreased sunlight temporarily by up to 10% even in distant locations.

To derive hourly solar insolation values from the insolation value of a given day and location, the radiation is distributed according to the daily pattern of its theoretical maximum, the clear sky value (CSV). The daily pattern of the CSV is proportional to the cosine of the declination of the sun over a given site during a given day [33]. The CSV is then multiplied with the daily insolation value divided by the integral over the CSV of that day [10]. The resulting pattern mimics the actual hourly distribution; it gives radiation beginning at sunrise in that location, peaks at noon local time, and ends at sunset. The integral of this distribution over one day is equal to the insolation for that day from NASA Surface meteorology and Solar Energy.

This distribution needs the lowest amount of electricity from storage; but it gives the actual pattern of radiation only on those days were insolation is equal to the maximum for that day. The pattern of actual radiation can be very different on days were insolation is considerably below the possible maximum for that day. For example, if insolation is only 50% of that maximum for two consecutive days, all radiation on day 1 could arrive during the first half of the day, and all radiation of day 2 could arrive during the second half of the day. To calculate an upper bound for storage under worst-possible patterns of insolation, we use pairs of two consecutive days where the total insolation of day 1 is fed into the system at sunrise on day 1 and the total insolation of the next day is fed into the system at sunset of day 2. Such a (hypothetical) situation would require more storage than situations in which the insolation patterns on both days are characterized by dramatic short-term fluctuations, such as those described by Apt et al. [34]. Hence, this provides an upper boundary for the required storage. Fig. 1 shows these upper and lower boundaries for the Mojave, a network consisting of the three North American deserts (NA3) and a Pan-American network. The minimal and maximal necessary storage values are similar for all three cases, while there are much larger differences across different locations and configurations.

In the following, a pair (G, S) is called "feasible" if it meets a 1 MW load continuously during 1986–2005. As locations differ in

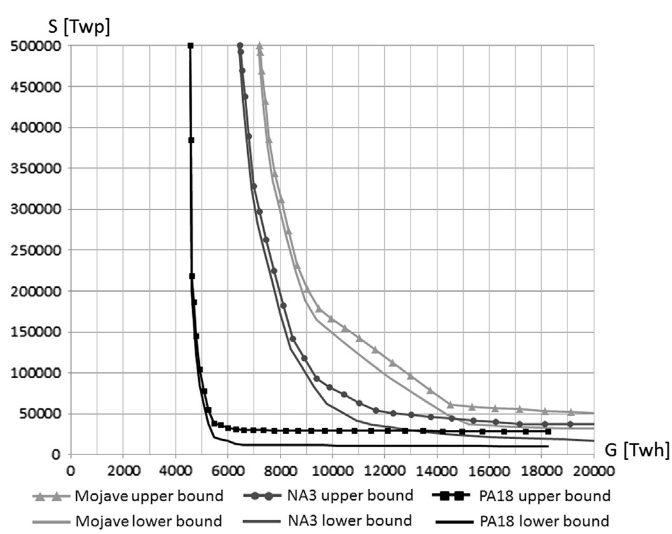

Fig. 1. *G*–*S*-Isolines for three locations/configurations (Mojave, NA3, and PA18) with insolation regimes as described in the text. The three isolines for minimal storage demand, in-between demand and maximal demand are similar to each other for each location/configuration.

their load pattern, a comparison of locations is easier if a constant load is used. As shown in [10], this method works equally well with varying load patterns. For calculation of the first feasible pair (G_1, S_1) of a *G*–*S*-Isoline an initial low value G_1 is found through optimization using a very high amount of storage (e.g., $S=$ 500 MW h). This value is sufficient for meeting a load of 1 MW for 20 days without insolation. The other points of the *G*–*S*-Isoline are calculated using progressively higher *x*-values, i.e. $G_{i+1} = a\,G_i, i = 1, 2, \ldots, a \in [1.023\%, 1.15\%]$ for calculation of the *y*-value S_{i+1} such that (G_{i+1}, S_{i+1})form a feasible pair with minimal S_{i+1}. Using daily insolation data from NASA Solar Sizer for 1986–2005, we find an Isoline-relationship for 72 locations all over the globe that we have tested, as well as for combinations of sites. We also find that the Isoline-relationship holds for hourly insolation values for locations in the US using the National Solar Radiation Database 1991–2010 Update [16].

4. The Solar Grand Plan revisited

The Solar Grand Plan was first introduced by Zweibel et al. [1], with additional analysis presented by the same team in [15]. For 2050, Fthenakis et al. [15] assume 6.7 terawatt (TW) of generation capacity to meet 35% of a projected energy demand of 3.1 TW i.e. 1.1 TW. In the Solar Grand Plan [1,15] *G* is composed of 2.54 TW CAES-PV (PV filling compressed air energy storage, CAES), 258 GW distributed PV, 1.5 TW CSP plants with thermal storage, 279 GW wind energy with CAES, 200 GW geothermal power. Adding up these capacities, taking into account the respective capacity factor of each capacity, gives a PV equivalent of 6.7 TWp. Auxiliary gas fired boilers in the CSP can provide 0.45 TW detachable energy; geothermal energy provides another 0.18 TW of firm electricity so that in extreme situations storage has to meet a remaining load of 0.47 TW load.

The Grand Plan [1,15] uses two types of storage, thermal storage together with CSP, and CAES. Storage has two main characteristics, its capacity and the power it can deliver. The thermal storage uses the turbines and generators of its CSP plant and thus gives the same power as that plant. CAES allows large storage capacity at low costs as it can, for example, use depleted caverns of natural gas, which may be very large. If caverns are used, the costs of CAES are not so much determined by the size of its cavern, but mostly by the size of its gas turbine plants and its generator, i.e. the power it can deliver, and by the low efficiency of CAES ($\sim$50%) which causes 50% losses that add to the costs. Almost all of the storage capacity of $\sim$258 TW h in Zweibel et al. [1] is in the form of CAES filled from PV with a storage time of up to 300 h.

Fig. 2 shows *G*–*S*-Isolines for an area of $1^\circ \times 1^\circ$ in the Mojave Desert and for a configuration of three North American deserts (NA3), each with loads of 0.92 TW (load of 1.1 TW minus geothermal) and 0.47 TW (load of 1.1 TW minus geothermal minus boilers), respectively. NA3 combines areas of $1^\circ \times 1^\circ$ in each of the three great deserts in North America (Mojave, Chihuahuan and Sonoran). The Isoline for NA3 uses the average insolation in these three deserts, as it would link solar parks in these three deserts. The values derived with Isolines for the Mojave Desert are very similar to the values calculated by Fthenakis et al. [15] using 45 years of data. The Isoline for NA3 shows that if these three deserts are combined, considerably less *G* and *S* are required compared to the Isoline for the Mojave Desert alone. This is valid for all feasible pairs of (G, S). Three different feasible pairs for $G = 6.7$ are marked, one on each isoline. The first is the value of (6.7, 258) as used by Fthenakis et al. for the Solar Grand Plan [15]. The second is the minimal feasible pair according to our method if no boilers are used (6.7, 217)—a 20% decrease in the required storage. If boilers

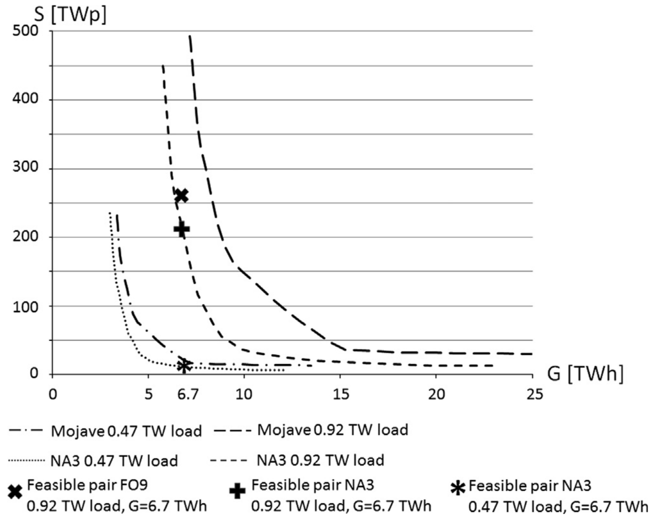

Fig. 2. *G*–*S*-Isolines for a $1^\circ \times 1^\circ$ area in the Mojave Desert and configuration NA3 consisting of $1^\circ \times 1^\circ$ sites in the Mojave, Chihuahuan and Sonoran, each with loads of 0.92 TW (no burners) and 0.47 TW (with burners) during 1986–2005. Three different feasible pairs for $G=6.7$ are marked, the pair (6.7, 258) as used by Fthenakis et al. [15], and the minimal feasible pairs according to our method without boilers (6.7, 217) and with boilers (6.7, 12).

are used all the time, the minimal feasible pair decreases to (6.7, 12).

Thus, boilers can meet almost 50% of the load. This is a high amount of spare capacity. Boilers provide ~3% of the total electricity but consume ~11% of the total energy at an efficiency of only ~30%. This low efficiency is due to the need for boilers to be cheap so that their fixed costs are acceptable. Providing 3% of the total electricity means that they are used for about 3% of a year. Even if their costs are as low as just ~30% of normal gas turbine power plants, their low usage rate still causes high costs of this electricity, more expensive by a factor of $100/3 \times 0.3 - 10$ (100%/3% × cost factor 0.3) which shows that the well-known problem of high costs of peak load also exists in this configuration. 3% of the electricity at 10 times the cost increases average costs of all electricity by 12.7%.

In the Grand Plan [1] demand is calculated with an annual net increase of 1%. Due to the higher future efficiency in the generation of energy enabled by renewable technologies, this implies an annual demand of 27,255 TW h or 3.1 TW in 2050, down from 29,307 TW h or 3.34 TW in 2020. Most of the increased efficiency is due to the characteristics of solar energy. For example, in the US 40% of the primary energy (1.2 TW) is used for generation of electricity with an average efficiency of 30%. Hence, 1.2 TW of primary energy give about 0.36 TW of electricity. Generating these 0.36 TW from solar would decrease primary energy demand from fossil energy by 1.2 TW. The net effect would be a decrease of total energy consumption by 0.84 TW (27%) to 2.26 TW.

The plan requires a cumulative subsidy of $420 billion until 2050. This is about double the global investments of $212 billion into renewable energy technologies in 2010 [35]. Could production of PV panels allow the completion of this plan? PV can only make a major contribution to the US energy supply if production volumes of PV panels increase considerably. Meeting the total global energy demand of 14 TW (i.e. all energy, not just electricity) requires an increase of current global manufacturing by a factor of ~100 [36]. At the average global growth rate of the last 35 years (doubling every 2 years) it would take 18 years to achieve 14 TW; at the lower growth rates of [37] it would take until 2050. All of these growth rates allow a major role for PV.

Like the Desertec EUMENA plan, the Solar Grand Plan assumes the construction of new ultra high voltage direct current (HVDC) power transmission networks. With the recent completion of the first very long distance HVDC lines in 2010 [38–40], further rapid cost decreases in long distance lines are expected from the combined effects of learning and economy of scale [12].

4.1. *Storage and overcapacity costs*

The calculation in the Grand Plan includes 20% electricity losses. Kymakis et al. [41] calculate losses of 38.3%, taking into account transformers, inverters, the panel temperature gradient, dust on panels and losses in transmission lines. Since the publication of the Grand Plan [1] and Kymakis et al. [41] most of those losses have decreased considerably. In 2011 losses of inverters produced by SMA, the leading company in this field, were down to 1–2.5% from previous 10–20% [42]. Additionally, as PV gives DC, no inverter from DC to AC is needed for DC transmission [36,39,43] so that inverters are only needed at the end of the line. All recently proposed large-scale schemes see DC (or superconducting) as standard in long-distance grids. Presently, the loss factor of 20% as assumed by Zweibel [28] appears more adequate, but now taking into account all factors listed in [41] updated to present values.

The Grand Plan predicts costs of 5.3 ¢/kW h, including losses of 20%. Updating these projections using [28,18] gives costs of 3.8 ¢/kW h for 2018 at an annual insolation of 2200 kW h/m^2, including 20% losses, which is considerably below the projections in the Grand Plan [1]. Transmission costs between deserts in South and North America with a line length of 7000 km are about 2 ¢/kW h at 100% line utilization including losses (based on [12]). With feasible utilization of 60% (see below) transmission costs would be 2.8 ¢/kW h (with losses corresponding to 60% utilization). This gives total costs of electricity of 6.6 ¢/kW h in 2018.

However, these costs increase for a North American solar scheme through the large required overcapacity. In 2050, the boilers will consume 11.7% of the total energy consumption. Both, the boilers and their fuel considerably add to costs, as outlined above for the capacity. The efficiency of CAES is 50–70%—with the upper end values being for adiabatic CAES where the heat from compressing the air is used within hours. Thermal storage has considerably higher efficiency. Hence, Fthenakis et al. [15] also employ CSP, which – though it is now much more expensive than PV – is well suited to thermal storage. Thermal storage is cheaper than CAES because heat is stored directly. Thermal storage at Spain's three Andasol 50 MW CSP plants is very good for about 7.5 h and acceptable for up to 16 h [44]. CAES allows much longer storage times at low losses but with conversion losses of 50%.

In 2100, the Grand Plan would meet a demand of 4.7 TW. The ratio between this demand and the capacity needed to generate this electricity (16.73 TW) gives the overcapacity in summer of about 3.5. This yields costs of $(3.5 - 1) \times 3.3$ ¢/kW h plus 3–5 ¢/kW h for storage as assumed by Fthenakis et al. [15], for total costs between 11.25 ¢/kW h and 13.25 ¢/kW h for electricity from storage. 70% of this capacity is only needed during winter; at other times this capacity generates excess electricity (which Fthenakis et al. [15] use for production of hydrogen, but the hydrogen plants would be idle to half idle during almost 6 months so that the hydrogen produced will be very expensive).

If the costs of PV and CSP drop to 2 ¢/kW h, which would be extreme, total costs would be 4 × 2 ¢/kW h plus 1–2 ¢/kW h given in the Grand Plan [1] for transmission, i.e., 8 ¢/kW h to 9 ¢/kW h, or 11 ¢/kW h to 14 ¢/kW h if storage is also included.

4.2. *Reviewing the Grand Plan for rapidly changing cost structures*

The feasible pair (6.7, 258) in Fig. 2 as used by Fthenakis et al. [15] is located in an area of a steep decline of the *G*–*S*-Isoline, indicating a rapid decrease of necessary *S* for a minor increase in *G*. For example,

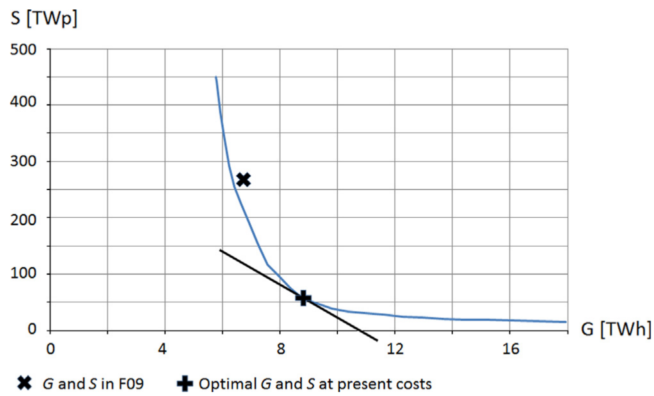

Fig. 3. *G*–*S*-Isoline and cost optimization for NA3 with a 0.92 TW load. Using more *G* and less *S* ("optimal *G* and *S* at present costs") decreases the costs compared to the situation in 2009 when Fthenakis et al. [15] was published ("*G* and *S* in F09").

increasing *G* from 6.7 to 9, i.e. by ~33%, would decrease the necessary *S* to about 20% of its former value from 258 to 53. This indicates the value of *G*–*S*-Isolines for the initial assessment of different options. Storage costs depend on the type of storage, their costs by capacity, power, efficiency, and utilization rate [45]. In actual applications a combination of different types of storage will be used, which is also suggested in the Grand Plan. Isolines are particularly helpful because due to technological progress and respective competitiveness, learning for *G*, *S* and transmission lines is different. Whereas costs of *G* decrease rapidly given learning, costs of *S* are changing much slower. The costs of HVDC transmission lines might decrease considerably since this is a new technology. *G*–*S*-Isolines allow fast evaluation of the effects of the rapidly diverging cost differentials between *G* and *S* (Fig. 3).

When the Grand Plan was published [1,15], PV and CSP could both generate electricity for 18 ¢/kW h. Costs for thermal storage of CSP were 1 ¢/kW h, costs of CAES for PV and wind power were assumed to be 4 ¢/kW h. This gave lower costs of electricity from CSP with thermal storage compared to PV with CAES. In 2013, the costs of PV have fallen to 8 ¢/kW h and the costs of CSP are still ~18 ¢/kW h, while the costs of storage have not changed much. This implies a considerable cost advantage for PV. Thus the ratio of the costs of PV per kW h to costs of CAES storage per kW h has changed from 18:4 in 2008 to 2:1 in 2013. The optimal ratio of *G* to *S* with 2008 costs can be found by parallel shifting the line with the slope $-18/4$; for 2013 the slope is $-2/1=-2$ (Fig. 3). As costs of PV could decrease further, the cost-optimal feasible pair (*G*,*S*) could move further down and to the right on the Isoline.

For the evaluation of the relative performance of configurations we used a simple synthetic cost index C_N for network *N*defined as $C_N = a\,r\,G + b\,S$, with *a*, *b* costs per unit of *G* and *S*, respectively (in MWp and MW h, respectively) and *r* is a parameter for testing the effect of a decreasing (or changing) cost ratio of *G* to *S*.

5. The Pan-American extension

Usage of large amounts of storage solves the problem of intermittency; use of excess electricity for hydrogen production decreases the problem of excess electricity, and auxiliary gas fired boilers decrease necessary generation capacity in winter. All of these options are necessary due to the northern winter and all are expensive. *G*–*S*-Isolines show that linking suitable North and South American sites can significantly reduce all types of intermittency–intermittency due to the cycles of day and night, weaker and shorter solar radiation during winter, and attenuation from weather. Connecting time zones decreases the effects of day and night; connecting both hemispheres compensates the winter in one hemisphere with the summer in the other hemisphere. We find that including tropical sites further reduces intermittency.

We analyze the design of a Pan-American extension through a comparison of networks with different types of sites: desert, arid or high insolation sites in North and South America, the three large deserts in North America, a site each in Florida and Texas, sites in or adjacent to the northern and southern Atacama desert, and three tropical sites in South America. We include sites at more poleward latitudes as these have high and long summer insolation. Table 1 lists all sites with their average annual insolation values on the horizontal plane (from [17]).

With insolation exceeding 2000 kW h/m^2 for all sites equatorward of 40°N/S latitude (with the exception of the site in Florida), the selected sites are well suited for both PV and CSP. The Atacama Desert has the lowest amount of rainfall worldwide and up to 20% higher insolation than the Mojave. The Sechura at 6°S experiences very little variation in insolation and length of day, with 12:25 h of sunlight in December and 11:35 h in June. It is not affected by snowfall, in contrast to subtropical locations like the Mojave or Atacama. Including the semi-arid Caatinga at 6.4°S increases the number of time zones in a configuration; this region could provide electricity 2 h earlier than the Atacama, 4 h earlier than Texas and 5 h earlier than the Mojave. Adding capacity in the Caatinga can markedly decrease the necessary *S*, see below.

To compare the value of different types of sites – high-latitude, subtropical desert, and tropical – we consider eight configurations (Table 2), including the previously considered NA3 and several Pan American configurations. The configuration "99 Locations" comes about if numerous solar installations on roofs and walls are added to the network that consists of all sites considered (PA-All). Such a development of residential solar installations appears highly likely and is only partially subject to considerations of overall optimality [22].

Fig. 4 shows insolation over two days during each season for the sites in the Mojave, Atacama, and Caatinga. Fig. 5 shows the

Table 1
The 18 locations in the US, Mexico (MX) and South America with geographical position and annual insolation in kW h/m^2.

Location	Position		Insolation
North America			
Deserts in North America			
Chihuahuan desert (US; MX)	31°N	108°W	2150
Mojave Desert (US)	36°N	117°W	2300
Sonoran desert (US; MX)	32°N	113°W	2180
North American regions with high insolation			
Florida	29°N	83°W	1840
Texas (US)	32°N	102°W	2020
North American regions at higher latitude			
Alaska Panhandle	58°N	134°W	1650
Koyukuk/Alaska	66°N	153°W	1720
South America			
Deserts in South America			
Atacama north (Chile)	19.5°S	69.5°W	2360
Atacama south (Chile)	24°S	69°W	2650
Bolivia Litoral	19°S	67°W	2290
Atacama further south (Chile)	27°S	69°W	2700
East of Atacama (Argentina)	24°S	67°W	2500
Catamarca (Argentina)	27°S	67°W	2430
North of Atacama (Peru, Interoceanica Sur)	17°S	70.5°W	2300
Tropic areas South America			
Caatinga (Brazil)	6.4°S	38°W	2080
Sechura I (Peru)	6°S	80°W	1980
Sechura II (Peru)	8°S	79°W	2100
South American region at higher latitude			
Santa Cruz (Argentina)	55°S	69°W	1125

Table 2
Sites included in the eight configurations and their basic characteristics.

Configuration		Sites (see Table 1 for details)	Sites	Longest nighttime (h)	Max. and min. daily insolation
1	NA3	3 North American deserts	3	14	9.05 1.05
2	NA5	NA3 and the two high insolation sites	5	12	8.48 1.27
3	NA7	NA5 and the North American higher latitude sites	7	12	8.0 0.98
4	PA6	NA3 and Atacama south, Bolivia Litoral, Catamarca	6	9	7.3 3.1
5	PAT	PA6 and two tropical sites: Caatinga, Sechura I	8	8	7.15 3.41
6	PAS	PAT and southern extension: Atacama north and further south, Sechura II	11	8	7.31 3.94
7	PA-All	All sites from Table 1	18	7 (see text)	6.51 3.85
8	99 Locations	PA-All plus roof and wall solar installations across the Americas	99	n/a	n/a

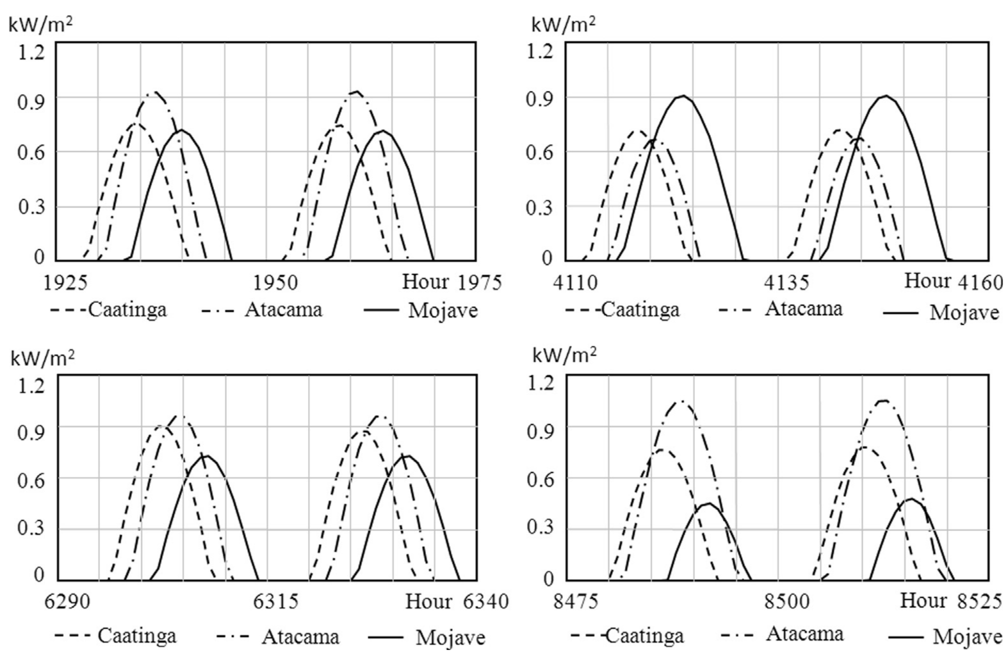

Fig. 4. Comparison of insolation in kW/m^2 in three locations for two consecutive days (50 h) during the four seasons: March 21st (top left), June 21st (top right), September 21st (bottom left), December 21st (bottom right).

insolation over one year in the Mojave, the Atacama, and their average. For the configuration that combines the Mojave with the Atacama, the ratio between the minimum and maximum over 20 years of insolation is reduced to 0.51, compared to 0.11 for the Mojave alone and 0.2 for the Atacama. The evaluation over twenty years shows that without tropical and low-lying hot deserts, problematic outages occur from rare attenuation events. Inclusion of tropical arid areas and deserts reduces occurrences of extreme peak-demand as well as the required long-term *S*.

Fig. 6 shows the calculated daily pattern of insolation, charging and use of storage over 50 h for all four seasons for the combination of NA3 with the three South American deserts (PA6 in Table 2). This figure also shows, that generation of electricity in this configuration is remarkably similar throughout a year. Here we use a constant load of 1 MW for easier comparison. *S* can be lowered to 12 MW h, i.e. sufficient for 12 h of consumption which is very low as compared to minimum storage sufficient for 235 h of load for the feasible pair in the NA3 configuration. Somewhat higher *S* seems reasonable as a safeguard. The longest nighttime in NA3 is 14 h in the northern winter. Linking the three North and three South American deserts (PA6) shortens the longest nighttime by 5 h to 9 h. Inclusion of the Caatinga site shortens the longest nighttime to 8 h. Combining all locations (PA-All) decreases duration of the longest night (in northern winter) to 7 h. There is always solar irradiance during the northern summer (values >0 but below 0.2 kW/m^2 for 5 h); peak values are above 12 kW/m^2.

In NA5, which links the five North American sites, average daily insolation varies between a daily minimum of 2.98 $kW\,h/m^2$ in December and a maximum of 7.1 $kW\,h/m^2$ in June, corresponding to a ratio of 42%, whereas the extremes through the 20 years have a ratio of 1.1 to 9.1 or 12%. By contrast, PA6, which connects the three North and three South American deserts, has a minimum average daily insolation of 5.6 $kW\,h/m^2$ in January and a maximum of 6.4 $kW\,h/m^2$ in April, corresponding to a ratio of 87.5% and a ratio of 3.1 to 7.3 or 42% for the 20-year extremes. Adding

the two tropical sites further improves the ratio of the long-term averages of maximum and minimum to 90% with an average daily insolation minimum of 5.6 kW h/m^2 in January and a maximum of 6.21 kW h/m^2 in October. PA-All (the combination of all sites considered) allows a slight further improvement with a minimum of 5.0 in January, a maximum of 5.52 in October, a ratio of 91%, and a ratio of 3.85 to 6.51 or 59% for the extremes.

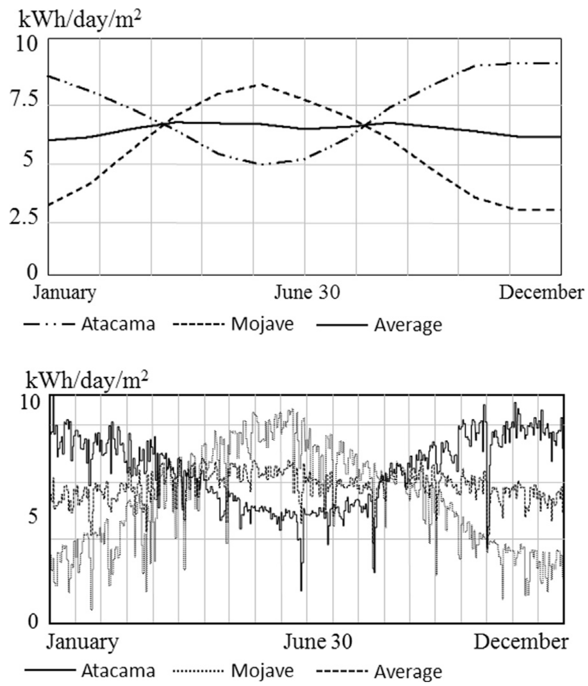

Fig. 5. Top: 23-year average of daily insolation in kW h/m^2 in the Atacama and Mojave and the average of the two locations (data from [17]). Bottom: Actual insolation for one year (1986).

5.1. Demand projection

For 2100, Fthenakis et al. [15] project a decrease in primary energy demand due to the higher efficiency resulting from the transition to sustainable electricity. A demand of 4.7 TW in 2100 for the US as assumed by Fthenakis et al. and a similar development in Canada gives an annual energy demand of 5.2 TW, or 41,000 TW h for the US and 5000 TW h for Canada.

Line utilization depends on economic growth in South America. For a scenario with high energy demand in South America we assume an average annual economic growth in South America during 2010–2100 of at most 4%. Growth of 4% yields a ratio of 1.6:1 between the North and South American economies until 2100, i.e. a demand of 28,750 TW h for South America (including Mexico). This gives a total projected demand of 74,750 TW h for North and South America together, corresponding to a capacity of 8.5 TW. From an energy unit cost perspective, higher growth rates than 4% per year would be better, as a ratio close to 1 between North and South America increases the utilization rates of transmission lines, which will decrease costs.

5.2. Long-distance transmission

In the Solar Grand Plan HVDC lines are preferred because these offer significant cost savings over long distances relative to conventional AC or lower voltage DC [36]. There are no capacitive, inductive or dielectric losses. Recently, transmission losses have decreased to 2–3% per 1000 km for 800 kV DC [24,36,46].In addition, investment costs for the lines are lower. Given much narrower tracks, necessary right of way is also considerably decreased.

The number of very long distance lines needed for a Pan-American network depends on cooperation between countries, their economic growth, reliability standards, and the development of transmission technology. Line costs depend on factors such as costs of labor, right of way, capital cost, line redundancy, terrain

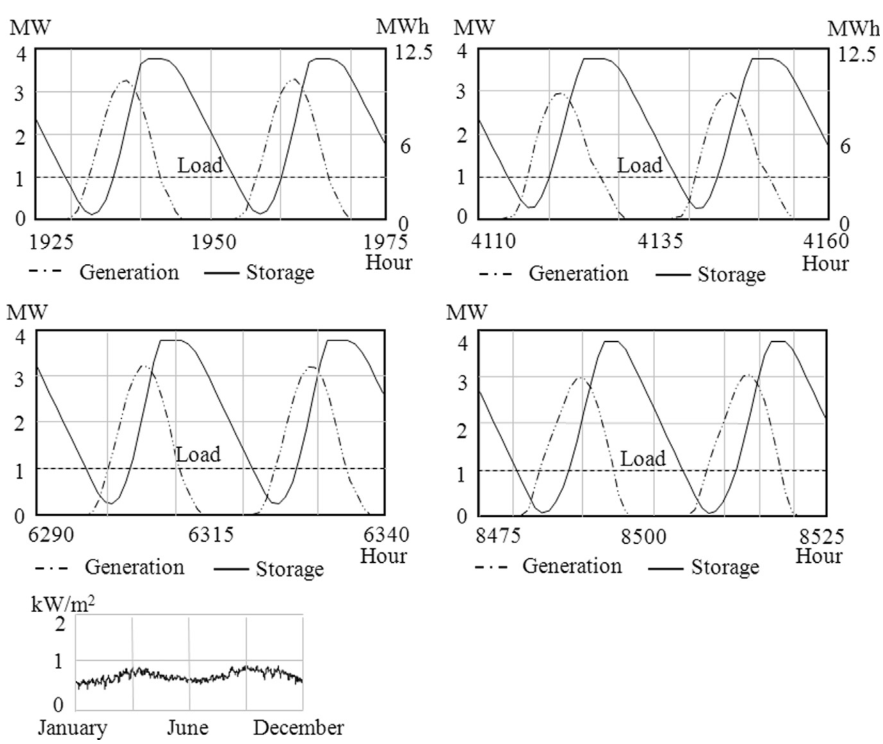

Fig. 6. Calculated daily pattern of insolation, charging and use of storage over 50 h for the four seasons for the combination of NA3 with the three South American deserts (PA6 in Table 2). Generation and load are in MW (scale on left), storage is in MW h (scale on right).

and land cover, and life expectancy of the lines. The highest demand for electricity from the Southern Hemisphere would be during northern winter when North American electricity generation is at 1/3 of generation during summer. If the projected North American demand of 5.2 TW were to be supplied with solar energy, 2/3 or 3.5 TW would need to come from South America. At the present transmission capacity of 6 GW per line, 580 cross-hemisphere HVDC lines would be needed. Transmission lines at 1500 kV are now discussed [47] which would increase capacity by a factor of $(1500/800)^2$ or 3.5 and decrease transmission costs per kW h by 17% [47]. A network between the two hemispheres would need 165 such lines.

Lines would need to connect and cross a number of countries. Some lines might be submarine or underground. Costs for underground cables are now similar to costs of overhead lines [12]; Table 3. Cost of electricity loss in lines, currently between 2% and 3% per 1000 km and station losses of around 0.6% [12,43], add considerably to transmission costs. Costs of losses depend on electricity costs; electricity costs from the Atacama are ~20% lower compared to the deserts in North America. The direct distance between the US grid of the Grand Plan and the closest Southern Hemisphere desert is 5900 km. Extrapolation of the data from [12] for a longer line of 8300 km gives transmission costs of ¢3.2/kW h. Significant cost differences are expected for the right of way. Transmission costs will further depend on the effect of learning as more long-distance lines are installed.

5.3. Learning curves for transmission costs

In 2010, only two very long distance high capacity DC transmission lines had been completed [39,40]. Thus, cost decreases due to learning will be significant. This can be described by learning curves which give the relative manufacturing costs as a function of the number of doublings in the volume of production, $C_0\alpha^n$, where C_0 is the initial cost of the line including stations and other electronics, and n the number of doublings of manufacturing capacity. $0<\alpha<1$ describes the decrease in manufacturing costs per doubling of manufacturing. We estimated earlier that 580 lines may be necessary to link North and South America. In addition, lines that connect in east–west direction will be needed. Installation of between 200 and 1000 lines means between seven to nine doublings from currently 2 lines. The learning curve for manufacturing costs as a function of the number of doublings is given as:

$$c_1(t) = c_0 a^{(\ln(M(t)/M_0)/\ \ln(2))} + F \qquad (1)$$

where $c_1(t)$ describes the cost in year t, c_0 the cost in year 2011 (the first year for which the number of doublings was available), $0<a<1$ is the learning coefficient, $M(t)$ the manufactured transmission capacity in year t (in GW), M_0 the capacity in year 2011 and F is the footing giving minimum costs of manufacturing a standard transmission line due to costs of material and a minimum amount of labor for production and installation. The smaller a, the faster the learning. PV with exceptionally rapid decrease of manufacturing costs has a learning coefficient $a=0.8$ [48,49]. Transmission lines will have considerably slower learning, because PV is a semiconductor technology and no other industry has shown a comparably fast exponential progress.

Fig. S1 shows the development of three different learning curves with a low speed of $0.05+0.95^n$, a middle speed of $0.12+0.88^n$ and a rapid speed of $0.22+0.78^n$. Based on the resulting costs E, the levelized transmission costs L_c per kW h are calculated with the standard formula for amortization

$$L_c = E \times A/(8760 \times U) \qquad (2)$$

with expenditures E, amortization coefficient A for a 40 year equipment lifetime and utilization factor U(division by 8760 converts to kW h). Our equipment lifetime estimate is on the careful side; Delucchi and Jacobson [50] indicate lifetimes between 50 and 70 years. The coefficient A is between 0.058 for a capital interest rate of 5% and a 40 year life expectancy of the equipment, 0.075 for an interest rate of 7% and a 40 year life expectancy, and 0.106 for an interest rate of 10% and a 30 years life expectancy. The example in [51] uses the latter values; we use 7% and 40 years. Other costs that have to be added are for operation and maintenance; these may be around 1% of the line costs.

Table 3 gives cost estimates for transmission, also with cost reduction due to learning, and distances in a Pan-American network. The shortest is a link between San Diego and the Sechura, an atypical desert in the tropics. Solar plants in the Sechura need to be connected to South American cities further south. The cost estimate based on data by ABB after completion of a 6 GW 800 kW DC line in China in 2010 [36] gives values very similar to those in [12]; station costs around $450–510 million are higher, but with twice the capacity. The losses (row 3) are calculated with 2% line loss, 0.6% loss in station and electricity costs of 7.5 ¢/kW h. As PV gives DC, only one station is needed, we add costs for a second station. As a long line needs the same number of stations as a short line, costs per kilometer are slightly lower for longer lines. The costs based on 2010 technologies under mid learning are in row 6; here for 60% utilization of the line.

5.4. Grid utilization

The utilization rate depends on the use of the line and the legal framework. For example, present North American reliability standards would require full redundancy of long lines. A transmission line that is used by only one solar plant has the same (usually low) utilization factor as the plant. The capacity factor of a solar installation is defined as the percentage of energy which this

Table 3
Transmission costs for overhead lines based on [24]; costs for underwater cables in brackets (from [12]).

	Distance [km]	2500	5000	7500	10,000	15,000	20,000
	Transmission costs (no learning, 100% utilization) [¢/kW h]	0.14	0.29	0.43	0.57	0.86	1.14
+	Costs of losses total at 7.5 ¢/kW h	0.47	0.87	1.22	1.59	2.34	3.09
+	Costs of 2 stations [¢/kW h]	0.13					
	Total costs [¢/kW h]	0.74 (1.0)	1.25 (2.0)	1.77 (3.0)	2.29 (4.0)	3.3 (3.6)	4.4 (4.6)
	Total costs (mid-learning rate, 60% utilization) [¢/kW h]	0.88	1.50	2.12	2.75	3.99	5.23
Distances between Southern hemisphere deserts and North America							
Line	Atacama south—San Diego	Piura (Sechura)—San Diego	Atacama—Caatinga	Paraiba (Caatinga)—San Diego (direct)	Paraiba (Caatinga)—San Diego (land)		
Length [km]	9557	7184	3850	9400	12,040		

installation gives during an average year compared to the energy it would give for uninterrupted insolation during all 8760 h of the year with 1 kW h/m^2. For example, with a typical capacity factor of 20–26% in southern California, line utilization from a solar park would also be between 20% and 26%. Low utilization increase transmission costs by several times.

If the long-distance transmission lines from South America were used only to send electricity to North America, the utilization rate could be as low as 25%, which increases transmission costs by a factor of 4. The maximum utilization rate is given by the difference between the two cosine distributions of insolation over a year on the respective hemispheres. It can become as high as 60% if solar plants on both hemispheres, distributed over most time zones in suitable areas in the Americas, are connected and electricity is sent in both directions. Additional use of S can further increase the utilization.

High utilization may be less important if the costs of a line are partially or fully paid from other sources. An important example is the sale of electricity to meet the peak load along the line, which can be highly profitable [12]. From the perspective of solar energy supply, the electricity imported during winter from the respective other hemisphere is peak electricity that meets peak load. Transmission lines, including east–west lines that connect the main grid with consumers, could also contribute to regional development, in particular in Brazil, Argentina, Chile, Columbia and Mexico, countries where economic growth has been linked to energy availability [53] or to renewable energy consumption [54]. Hence, line costs should also be evaluated in that context. For example, east–west lines from the Caatinga region through Brazil could support the economic development of the entire transect from the Atlantic to the Pacific. This line would have a total length of 14,000 km if connected to North America.

The grid should have adequate spare capacity to decrease vulnerability. If a politically instable country allowed the destruction of long-distance lines in a network with redundancy, it will be disconnected from a major source of its energy, whereas other countries will still get electricity via other lines in the network. Like today with major supra-national technical infrastructure it can be assumed that countries will be very careful to avoid interruptions in their territories.

6. Results

Table 4 gives values of G and S for the configurations described above if costs of electricity are minimized. Combining North and South American sites permits a dramatic reduction in the required G and S. Fig. 7 compares configurations in the Americas through their Isolines.

The two best Pan-American networks can meet the combined North–South American demand of 8.5 TW projected for 2100 with G between 54 TWp and 63 TWp and S between 101 TW h and 105 TW h. In terms of generation capacity G this is even slightly better than the capacity of between 63 TWp and 85 TWp that would be needed by a network consisting of just the three US Southwest sites to meet the load of 4.7 TW projected for North America alone.

Over a wide variety of values of r (from 0.5 to 8), the combination of all sites considered (PA-All) had the lowest cost index C_N. Almost the same cost values were possible with a network of only eight locations—the three North and three South American deserts and two tropical sites (PAT). The third lowest cost index was achieved by the network with all 99 locations, including rooftop and wall-based, throughout the Americas. A more precise cost estimate needs precise specifications which types of storage to use and how much of each type is needed in a specific network. However, as all Pan-American networks can do with very low amounts of storage, this restriction is not very rigid.

Thus, a Pan-American network can meet almost twice the demand than a North American network with a similar G. This advantage also exists in the need for storage, with minimal values of 110–113 TW h for a 4.7 TW load in the network of the three US Southwest sites, versus minimal values of 101–117 TW h for the Pan-American configurations and a load of 8.5 TW. The reduction in S, and in particular long-term S, enabled by a Pan-American extension points to perhaps the biggest problem faced by a US-based solar energy network. Due to the combination of low insolation and shorter days during winter, a North American solar network requires large amounts of expensive long-term storage,

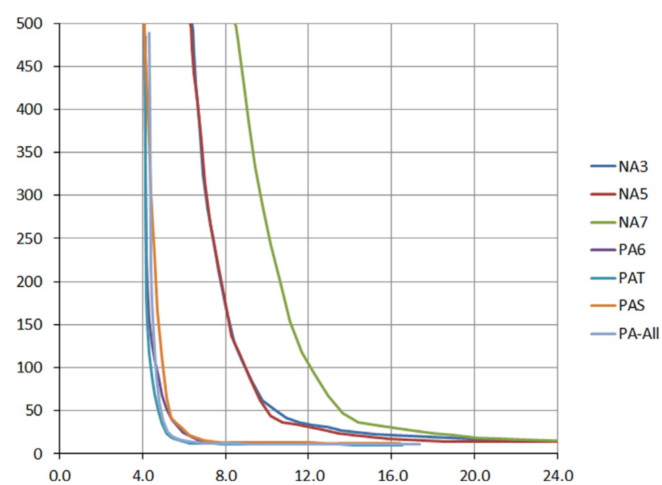

Fig. 7. Comparison of seven configurations in the Americas through their G–S-Isolines.

Table 4
Comparison of the G and S required for the eight configurations for a generic 1 MW load and for the projected load in 2011 of, respectively, 8.5 TW for the Americas and 4.7 TW for the US. n/a: not available.

Configuration	Cost optimal G and S (1 MW load)			Load 8.5 TW (Pan-Am)		Load 4.7 TW (U.S.)	
	G [MWp]	S [MW h]	Cost [kW h]	G [TWp]	S [TW h]	G [TWp]	S [TW h]
NA3	13.3	27.4	13.7	113	233	63	129
NA5	13.4	24.1	12.9	114	205	63	113
NA7	18	23.4	15.5	153	199	85	110
PA6	7.4	11.9	6.8	63	101	n.a	n.a.
PAT	6.3	12.3	6.3	54	105		
PAS	7.4	13.8	7.2	63	117		
PA-All	6.6	12.7	6.5	56	108		
99 Locations	7.9	11.8	7.1	67	100		

overcapacity and fuel. A combination of North and South American sites provides a natural solution to this problem.

With solar electricity costs of 4.7 ¢/kW h in 2030, and the estimated costs for transmission given above of respectively, 2.75 ¢/kW h, 2.1 ¢/kW h, and 2.2 ¢/kW h for transmission between San Diego and the Atacama, the Sechura, and the Caatinga total electricity costs of ~6 ¢/kW h, 5.7 ¢/kW h, and 6.1 ¢/kW h can be projected, taking into account a mix of 50% from the US and 50% from South America.

7. Discussion

A Pan-American network offers significant improvements with regard to fuel, capacity and storage over a US only network as proposed in the Solar Grand Plan [1]. The Grand Plan requires fuel on the order of 11.7% of the energy consumed, and high amounts of storage. Projected electricity prices from PV are 5.3–5.7 ¢/kW h by 2050 and 7.3–7.7 ¢/kW h with transmission costs. The network presented here does not require fuel and is able to meet the projected demand of the entire North and South American continent in 2100 with about the same capacity that is required for a North American network in order to meet only the projected North American demand. The estimated electricity costs without storage will be between 5.7 ¢/kW h and 6.1 ¢/kW h, which is less than the prices estimated by Zweibel et al. [1], despite the costs of long-distance transmission. However, the most important cost savings relative to the Grand Plan result from the dramatic decrease in expensive long-term storage. Given the high losses of long-term storage, such storage is responsible for a significant portion of the overcapacity in the Grand Plan [1].

A Pan-American solar energy network could help buffer against droughts in Brazil, where hydropower accounted for approximately 85% of electricity generation in 2009 [55]. In a warming world, average annual flow in basins used for hydropower generation is projected to decrease by 9–11% for approximately doubled CO_2 concentrations [56]. Large-scale availability of electricity could also support economic development in South America. The use of arid areas for agriculture provides only low income. Availability of electricity could support schemes that improve living conditions through education and local economic development, and through availability of cooling and appropriate storing for agricultural produce, processing of food, and desalination of brackish ground water. Hence, the costs of new long-distance transmission lines may also be attributable to regional development.

In a Pan-American network, each hemisphere provides a natural market for the excess electricity of the other hemisphere during winter. At higher penetration with solar electricity, line utilization would be limited by the difference in the size of the North and South American economies. The ratio of the North American GDP to the GDP of the rest of the Americas is currently 3.9:1. However, there is a considerable potential for economic growth, also given the ratio of population numbers, which is at 0.64:1. A 3.9:1 ratio would imply a utilization factor of approximately 40% as lines are used only at 12.5% in the north–south direction. Before a high penetration with solar electricity is achieved, the relative size of the economies in North America and South America may well be more similar. With storage in all locations, electricity could flow 24 h according to the respective load factors which may raise utilization above 70%. An important consequence is that electricity costs for North America will be progressively lower if South America develops well economically.

Acknowledgements

The first and third authors were supported by a research grant of the Austrian National Bank (Project No 14451, DEVELOP). The second author was supported by the Center for Climate and Energy Decision Making created through a cooperative agreement between the National Science Foundation (SES-0949710) and Carnegie Mellon University. The authors thank Brigitte Wolkinger for effective research support.

Appendix A. Supporting information

Supplementary data associated with this article can be found in the online version at http://dx.doi.org/10.1016/j.rser.2014.01.003.

References

[1] Zweibel K, James M, Fthenakis V. Solar Grand Plan Sci Amer 2008;298:64–73.
[2] Battaglini A, Liliestam J, Haas A, Patt A. Development of SuperSmart grids for a more efficient utilization of electricity from renewable sources. J Cleaner Prod 2009;17:911–8.
[3] Viebahn P, Lechon Y, Trieb F. The potential role of concentrated solar power (CSP) in Africa and Europe—a dynamic assessment of technology development, cost development and life cycle inventories until 2050. Energy Policy 2011;39:4420–30.
[4] Desertec. Clean power from deserts: the DESERTEC concept for energy, water and climate security. Desertec Foundation, Protext Verlag, Bonn, 2009.
[5] Desertec Industrial Initiative, 2012. EUMENA 2050: powered by renewable energy. Desertec Industrial Initiative, 16pp.
[6] Taggart S, James G, Dong ZY, Russel C. The future of renewables linked by a transnational Asian grid. Proc IEEE 2012;100:348–59.
[7] Trieb F, Schillings C, Pregger T, O'Sullivan M. Solar electricity imports from the Middle East and North Africa to Europe. Energy Policy 2012;42:341–53.
[8] Meisen P, Pochert O. A study of very large solar desert systems with the requirements and benefits to those nations having high solar irradiation potential. Global Energy Network Institute, 2006: 36.
[9] Jacobson MZ, Delucchi MA. Providing all global energy with wind, water and solar power, Part I: Technologies, energy resources, quantities and areas of infrastructure and materials. Energy Policy 2011;39:1154–69.
[10] Grossmann W, Grossmann I, Steininger K. Distributed solar electricity generation across large geographic areas, Part I: a method to optimize site selection, electricity generation, and storage. Renew Sustainable Energy Rev 2013;25:831–43.
[11] Hart EK, Stoutenburg ED, Jacobson MZ. The potential of intermittent renewables to meet electric power demand: current methods and emerging analytical techniques. Proc IEEE 2012;100(2):322–34.
[12] Chatzivasileaiadis S, Ernst D, Andersson G. The global grid. Renewable Energy 2013;57:372–83.
[13] Palmintier B, Hansen L, Levine J. Spatial and temporal interactions of solar and wind resources in the next generation utility. In: Proceedings of SOLAR 2008 conference and exhibition, San Diego, CA; May 3–8, 2008.
[14] Marcos J, Marroyo L, Lorenzo E, Garcia M. Smoothing of PV power fluctuations by geographical dispersion. Prog Photovoltaics Res Appl 2012;20:226–37.
[15] Fthenakis V, Mason JE, Zweibel K. The technical, geographical, and economic feasibility for solar energy to supply the energy needs of the US. Energy Policy 2009;37:387–99.
[16] Wilcox S. National solar radiation database 1991–2010 update: user's manual. National renewable energy lab technical report NREL/TP-5500-54824; 2012. Data available online at: ⟨http://rredc.nrel.gov/solar/old_data/nsrdb/⟩.
[17] NASA. Radiation Budget Data Products: SSE surface meteorology and solar energy data. NASA Applied Sciences Program; 2010.
[18] Maycock, P. 2013. In: The future of energy summit 2013. Bloomberg New Energy Finance. ⟨http://bnef.com/Presentations/download/136⟩.
[19] Breyer C, Gerlach A. Global overview on grid-parity events. Prog Photovoltaics Res Appl 2013;21:121–36.
[20] Martínez-Duart JM, Hernández-Moro J. Photovoltaics firmly moving to the terawatt scale. J Nanophotonics 2013;7(1) (2013).
[21] Bazilian M, Onyeji I, Liebreich M, MacGill I, Chase J, Shah J, et al. Re-considering the economics of photovoltaic power. Renewable Energy 2013;53: 329–38.
[22] Schleicher-Tappeser R. How renewables will change electricity markets in the next five years. Energy Policy 2012;48:64–75.
[23] Hand MM, Baldwin S, DeMeo E, Reilly JM, Mai T, Arent D et al. editors. Renewable electricity futures study. NREL/TP-6A20-52409, 4 vols. National Renewable Energy Laboratory, Golden, CO.
[24] Dufo-Lopez R, Bernal-Agustin JL. Photovoltaic grid parity in Spain. Adv Mech Electr Eng 2013;178:235–9.
[25] Li J. Scaling up concentrating solar thermal technology in China. Renewable Sustainable Energy Rev 2009;13:2051–60.

[26] Sims RE, Schock RN, Adegbululgbe A, Fenhann J, Konstantinaviciute I, Moomaw W et al. Energy supply. In Climate change 2007: Mitigation. Contribution of working Group III to the fourth assessment report of the Intergovernmental Panel on Climate Change 2007, Cambridge University Press.
[27] Roca M. First large solar plants without subsidy sought in Spain. Bloomberg; Dec. 21, 2012.: 〈http://www.bloomberg.com/news/2012-12-21/first-large-solar-plants-without-subsidy-sought-in-spain.html〉.
[28] Zweibel K. The terawatt challenge for thin-film PV. National Renewable Energy Laboratory; 2005. Technical report NREL/TP-520-38350.
[29] Budischak C, Sewell D, Thomson H, Mach L, Veron DE, Kempton W. Cost-minimized combinations of wind power, solar power and electrochemical storage, powering the grid up to 99.9% of the time. J Power Sources 2013;225:60–74.
[30] NASA. Surface meteorology and solar energy (SSE) release 6.0 Methodology; January 10, 2013. 61pp.
[31] Pinker R, Laszlo I. Modeling surface solar irradiance for satellite applications on a global scale. J Appl Meteorol 1992;31:194–211.
[32] Smith GL, Green RN, Raschke E, Avis LM, Suttles JT, Wielicki BA, et al. Inversion methods for satellite studies of the Earth's radiation budget: development of algorithms for the ERBE mission. Rev Geophys 1986;24:407–21.
[33] Milone EF, Wilson W. Solar system astrophysics: background science and the inner solar system. Springer; 2008.
[34] Apt J, Fertig E, Katzenstein W. Smart integration of variable and intermittent renewables. In: Proceedings of 45th Hawaii international conference on system sciences; 2012. 1997–2001.
[35] UNEP. 2011. United Nations Environment Programme and Bloomberg New Energy Finance, 2011, Global trends in renewable energy investment 2011. ISBN: 978-92-807-3183-5.
[36] Grossmann WD, Grossmann I, Steininger KW. Indicators to determine winning renewable energy technologies with an application to photovoltaics. Environ Sci Technol 2010;44:4849–55.
[37] Grossmann, W.D., Steininger, K.W., Schmidt, C.,Grossmann, I. Investment and employment from large-scale photovoltaics up to 2050. Empirica Special Issue 'Climate and Global Change, Selected Papers from the 2011 Annual Meeting of the Austrian Economic Association' 2012;39:165–189.
[38] ABB. Group. Ultra-High Voltage DC Systems. Pamphlet no POW-0043, ABB Limited; 2010.
[39] Åström U, Lescale VF, Menzies D, Weimin M, Zehong L. The Xiangjiaba-Shanghai 800 kV UHVDC project, status and special aspects. In: Proceedings of international conference on power system technology; 2010. 1–6.
[40] Breuer W, Retzmann D, Ueker K. Highly efficient solutions for smart and bulk power transmission of green energy. In: 21st world energy congress; 2010.
[41] Kymakis E, Kalykakis S, Papazoglou TM. Performance analysis of a grid connected photovoltaic park on the island of Crete. Energy Convers Manage 2009;50:433–8.
[42] SMA Solar Technology. SMA product guide: sunny family 2011/2012. SMA Solar Technology; 2011.
[43] Czisch G. Low cost but totally renewable electricity supply for a huge supply area—a European/Trans-European example. In: Proceedings of Jahrestagung der Deutschen Physikalischen Gesellschaft; 2006.
[44] Viebahn P, Kronshage S, Trieb F, Lechon Y. Final report on technical data, costs, and life cycle inventories of solar thermal power plants. German Aerospace Center, 2008.
[45] Irena. 2012. Solar Photovoltaics 1 (4/5, 2012).
[46] McCall J, Gamble B, Eckroad S. Combining superconductor cables and VSC HVDC terminals for long distance transmission. In: Proceedings of the IEEE conference on innovative technologies for an efficient and reliable electricity supply; 2010. 47–54.
[47] Huang H, Kumar D, Ramaswami V, Retzmann D. Concept paper on development of UHVAC system in India. Siemens AG, Germany; 2010.
[48] Trancik JE, Zweibel K. Technology choice and the cost reduction potential of photovoltaics. In: Proceedings of the IEEE world conference on photovoltaic energy conversion; 2006. 2490–93.
[49] Breyer C, Birkner C, Kersten F, Gerlach A, Goldschmidt JC, Stryi-Hipp G, et al. Research and development investments in PV—a limiting factor for a fast PV diffusion? In: 25th European photovoltaic solar energy conference and exhibition; 2010.
[50] Delucchi MA, Jacobson MZ. Providing all global energy with wind, water and solar power, Part II: Reliability, system and transmission costs, and policies. Energy Policy 2011;39:1170–90.
[51] Bahrman M. HVDC transmission. In: IEEE power systems conference & Exposition; 2006.
[53] Chontanawat J, Hunt LC, Pierse R. Does energy consumption cause economic growth? Evidence from a systematic study of over 100 countries J Policy Model 2008;30:209–20.
[54] Pao HT, Fu HC. Renewable energy, non-renewable energy and economic growth in Brazil. Renewable Sustainable Energy Rev 2013;25:381–92 (Energy Information Administration. Country Analysis Briefs: Brazil. Energy Information Administration 2011.).
[55] Energy Information Administration. Country Analysis Briefs: Brazil. Energy Information Administration; 2011.
[56] De Lucena AFP, Szklo AS, Schaeffer R, de Souza RR. Borba BSMC, da Costa IVL et al. The vulnerability of renewable energy to climate change in Brazil. Energy Policy 2009;37:879–89.